

Elastic and Inelastic Scattering of 13- to 19-MeV Protons by $O^{16}\dagger$

W. W. DAHNICK

Palmer Physical Laboratory, Princeton University, Princeton, New Jersey
and*Sarah Mellon Scaife Radiation Laboratory, University of Pittsburgh, Pittsburgh, Pennsylvania*

(Received 27 March 1964; revised manuscript received 11 May 1964)

Closely spaced differential cross sections have been obtained for elastic and inelastic scattering of protons by O^{16} ($0 \geq Q \geq -8.88$ MeV). At laboratory angles of 80, 100, 120, 140, and 160°, continuous elastic excitation curves over the energy range from 13 to 19 MeV were obtained by a thick-target technique. For proton energies between 14.8 and 19.2 MeV, additional measurements with about 200-keV energy resolution were made by conventional thin-target techniques. Numerical values of cross sections for elastic and inelastic scattering are presented for the angular range from 15 to 160° at typically 10° angular and 200-keV energy intervals. Differential cross sections often change by a factor of 2 within 200–500 keV for large as well as small angles. The largest resonance is found at 14.9 MeV, but fluctuations at the upper end of the energy scale (≈ 19 MeV), particularly for inelastic scattering, are not significantly smaller. Some, but not all, of these strong fluctuations occur slightly above the five reaction thresholds ($(p,2p)$, (p,d) , (p,He^3) , (p,pn) , (p,n)) in the 12- to 19-MeV region. Previously, nine of the elastic angular distributions reported here had been made available for analysis by the use of an optical-model search code. Fits to within 10% were obtained, but the optical-model parameters for good fits showed strong energy dependence. It is suggested that simple potential scattering provides an insufficient explanation for $O^{16}(p,p)O^{16}$ for the energy region investigated. The interference of potential scattering with compound nuclear scattering is discussed and shown to be very noticeable, even for 200-keV energy resolution. Data and analysis emphasize the need for a theoretical approach to scattering which takes explicit account of easily formed states in light nuclei.

I. INTRODUCTION

FOR heavy nuclei, the density of states of given spin and parity at several MeV excitation is so high that compound-nuclear contributions to proton scattering can either be calculated by statistical methods or safely ignored for low-lying states. For light nuclei, it generally is not permissible to neglect the compound contribution to scattering, even if the excitation of the compound system exceeds 15 or 20 MeV. Interference effects of “direct” and “compound” scattering amplitudes remain very noticeable. The intent of this work is to study cross section changes with energy for scattering of protons by O^{16} in detail and, if possible, to find the magnitude of the strongly energy-dependent part of the scattering amplitude for this particular nucleus and energy region.

Scattering of low-energy protons by O^{16} has been investigated repeatedly, and for energies up to 13 MeV very recent and detailed high-resolution excitation functions exist.^{1–3} Above 13 MeV, experimental data are much less complete and consist of a few angular distributions at different bombarding energies.^{4–8} $O^{16}(p,p)O^{16}$

cross sections for back angles are known to change rapidly with proton energy up to bombarding energies of at least 20 MeV.⁷ For low proton energies many narrow, $\Gamma < 100$ keV, resonances have been observed.^{1–3} At higher energies, e.g., between 8.5 and 13 MeV, most of the known resonances seem to have widths between 120 and 350 keV.^{2,3} It is, therefore, not unreasonable to expect that for energies above 13 MeV the energy resolution of cyclotron beams will suffice to reveal most of the strong resonances. The exact determination of their widths and the detection of narrow resonances, of course, would have to await the completion of high-energy, high-resolution accelerators.

The level density and the level widths in the compound nucleus (F^{17}) increase as the energy is increased, and fluctuations in scattering cross sections become shallower and broader. One might ask if, as in heavier nuclei, there is an energy in the 10–20-MeV region above which optical model and distorted-wave Born approximation (DWBA) scattering theories can correctly account for most of the scattering amplitude. In order to facilitate an answer to this question, differential cross sections were measured for relatively small angular and energy intervals. Most of the elastic angular distributions presented in this paper, together with lower energy cross sections obtained by Kobayashi,⁶ were analyzed by Duke⁹ with the UCLA optical-model automatic search program.¹⁰ Just as for the similarly analyzed

† This work was supported by the U. S. Atomic Energy Commission and the Higgins Scientific Trust Fund, and the National Science Foundation.

¹ S. R. Salisbury, G. Hardie, L. Oppliger, and R. Dangle, *Phys. Rev.* **126**, 2143 (1962).

² G. Hardie, R. L. Dangle, and L. D. Oppliger, *Phys. Rev.* **129**, 353 (1963); G. Hardie, Ph.D. thesis, University of Wisconsin, 1962 (unpublished).

³ R. L. Dangle, L. D. Oppliger, and G. Hardie, *Phys. Rev.* **133**, B647 (1964).

⁴ W. F. Hornyak and R. Sherr, *Phys. Rev.* **100**, 1409 (1955).

⁵ B. B. Kinsey and T. Stone, *Phys. Rev.* **103**, 975 (1956), and B. B. Kinsey, *ibid.* **99**, 333 (1955).

⁶ S. Kobayashi, *J. Phys. Soc. Japan* **15**, 1164 (1960).

⁷ D. R. Maxson, *Phys. Rev.* **123**, 1304 (1961).

⁸ Data for $O^{16}(p,p)O^{16}$ at $E_p = 31.0$ MeV, H. H. Forster (private communication).

⁹ C. B. Duke, *Phys. Rev.* **129**, 681 (1963).

¹⁰ M. A. Melkanoff, J. S. Nodvik, D. S. Saxon, and D. G. Cantor, *A Fortran Program for Elastic Scattering Analysis with the Nuclear Optical Model* (University of California Press, Berkeley and Los Angeles, California 1961).

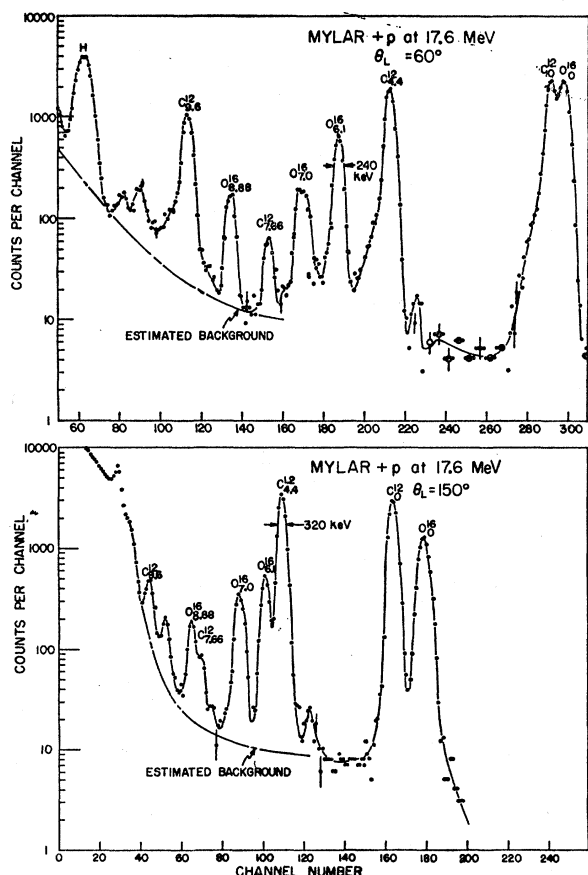


FIG. 1. Typical NaI scintillator pulse-height spectra of 17.6-MeV protons scattered from a thin Mylar target through 60° and 150°. Peaks are labeled by isotope and excitation energy. For $\theta_{lab}=60^\circ$ the shape of the 7-MeV group indicates comparable excitation of the 6.92- and 7.12-MeV levels.

$C^{12}(p,p)C^{12}$ scattering,^{11,12} all data above 12 MeV could be fitted for angles up to 160° to about $\pm 10\%$ or better; however, these fits could be obtained only at the cost of considerable and nonsystematic energy variation of some optical-model parameters. The difficulties with energy variation of parameters were worse for O¹⁶ than for C¹². This is consistent with the observation that the fluctuations of all O¹⁶(p,p')O¹⁶ cross sections are even more pronounced than the fluctuations in the $C^{12}(p,p')C^{12}$ cross sections for the same energy region.

II. EXPERIMENTAL METHODS

The inelastic and most of the elastic cross sections presented in this paper were obtained by conventional scintillation counter (NaI) spectroscopy. Commercial Mylar foils (C₁₀O₄H₈) served as targets and were always chosen to be thinner than 100 keV. At angles smaller than 60°, the C¹² and O¹⁶ elastic peaks were not resolved. However, reasonably accurate O¹⁶ cross sections could

¹¹ J. S. Nodvik, C. B. Duke, and M. A. Melkanoff, Phys. Rev. 125, 975 (1962).

¹² W. W. Daehnick and R. Sherr, Phys. Rev. 133, B934 (1964).

be obtained by measuring the $C^{12}(p,p)C^{12}$ cross sections immediately following or preceding each Mylar run with a polystyrene (C_nH_n) target. Apart from the necessary subtractions at small angles thin target O¹⁶ data were obtained and analyzed in a manner identical to that described for C¹² data in Ref. 12, and simultaneously with them. Mylar targets were preferred over a gas target because they permitted the combination of good angular resolution, easy absolute cross-section measurements, and high counting rates. Commercial chemical analysis of the Mylar foils used yielded a composition C₁₀O₄H_{8.3} plus negligible traces of heavier elements. The chemical analysis is believed to be accurate to 0.5% for carbon and oxygen and to 2% for hydrogen. The pulse-height resolution of the NaI(Tl) scintillation counters used was better than or close to 2% for 15-MeV protons. This resolution, however, is still insufficient to resolve the doublets at ≈ 7 and ≈ 6 MeV (see Fig. 1). At one energy (17.0 MeV) several spectra were taken with a 1-mm-thick gold surface barrier detector (Molechem, Inc.) which was mounted at an angle of 60° with respect to the proton trajectories. A 2-mm-deep sensitive region obtained in this manner stopped 17-MeV protons, and the improved resolution allowed an estimate for the cross sections of the 6.92- and 7.12-MeV states individually (Fig. 2). The energy resolution in these particular runs was about 145 keV

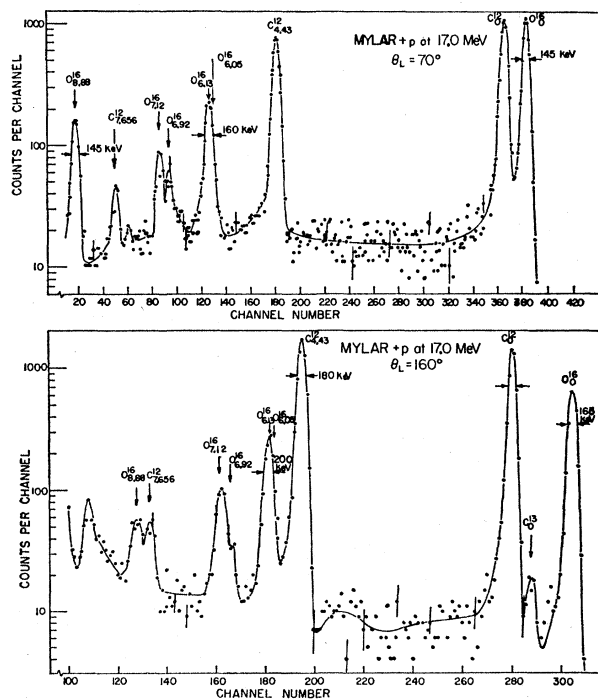


FIG. 2. Pulse-height spectra of 17-MeV protons taken with an early Au surface barrier (Si) detector. For $\theta_{lab}=70^\circ$ the 6.92-7.12-MeV doublet is resolved. Peak widths are essentially that of the beam width, except for the group at 6.1 MeV which appears slightly broader. The continuum "background" is due to elastic protons which lost only part of their energy in the depleted region.

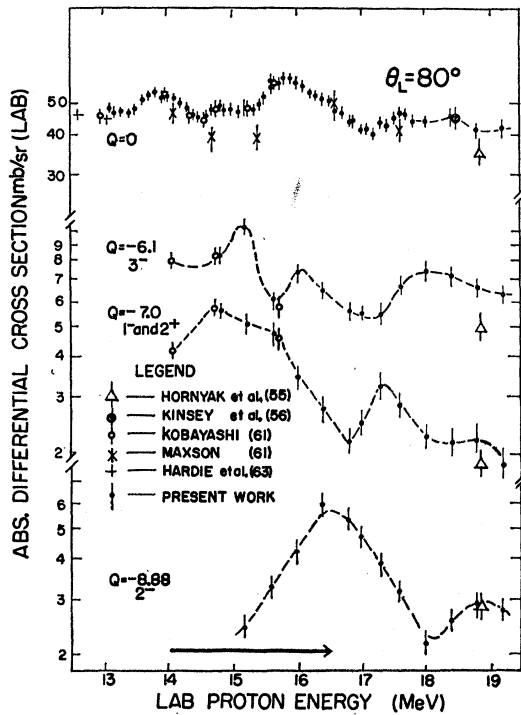


FIG. 3. Comparison of data presented in this paper for $\theta_{lab}=80^\circ$ with previously published cross sections. $\theta_{lab}=80^\circ$ corresponds to the second diffraction maximum for elastic scattering, and comparison with other publications is most sensitive to the calibration of the absolute cross-section scale. Differences in energy and angular resolution will have little effect on the agreement.

and mostly due to the energy spread in the cyclotron beam. The excitation energy of the 6-MeV group was measured as $Q = -6.1 \pm 0.020$ MeV and its width was 160 keV as compared to 145 keV for the 8.88 MeV and the elastic peaks. This suggests that the 6.05-MeV (0^+) state is still weakly excited in inelastic proton scattering at 17 MeV. (It is quite strongly excited below $E_p = 10$ MeV.³) In the cross sections given below the first four O^{16} levels are lumped into the 6.1- and 7.0-MeV groups, since only the sum of the cross sections for each doublet is known reliably.

Thick-Target Measurements

Previously a time-saving thick-target method¹² had been successfully used in this laboratory for the measurement of excitation functions. It was again employed for O^{16} with some degree of success, and we briefly review the experimental procedure: An oxygen target, about 2 MeV thick for the incoming beam, was placed at the center of the Princeton 60-in. scattering chamber. Scattered protons were observed with a NaI(Tl) scintillation counter at back angles (80 – 160°), while the target was positioned in such a way that the detected protons entered and left the target through the same surface. Thus the energies of the emerging, elastically scattered, protons varied greatly, depending on the depth (and,

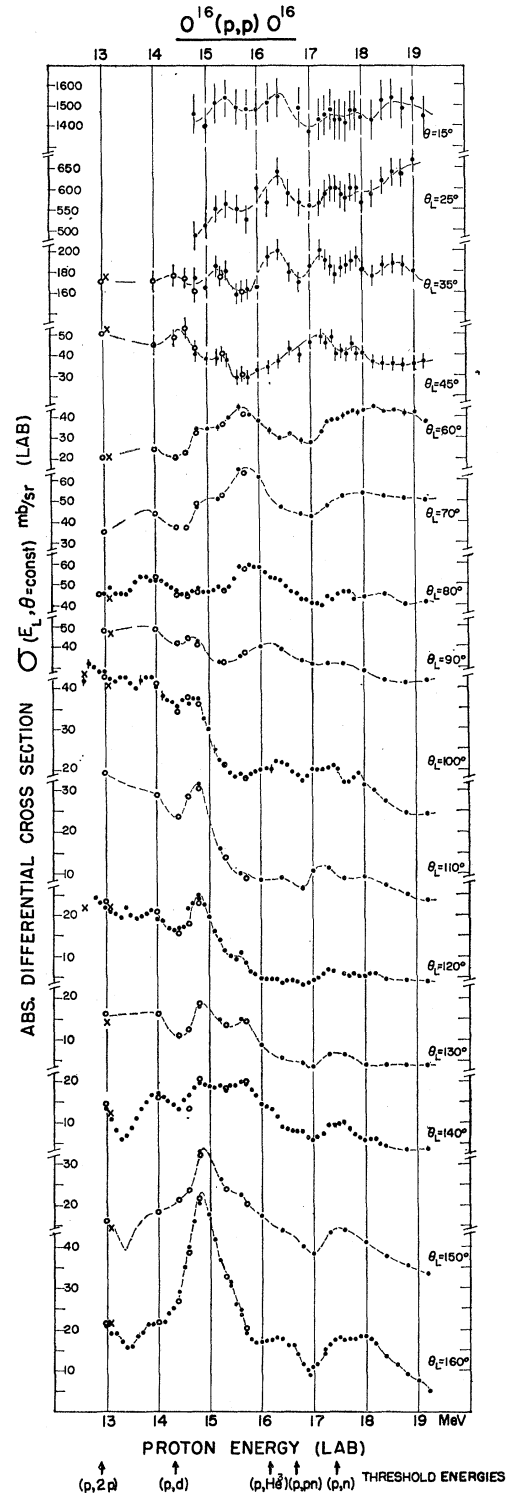


FIG. 4. Present elastic-scattering data presented as excitation functions for proton energies from 13 to 19 MeV (solid dots). Open circles are data taken from Ref. 6 and plotted at 100 keV higher energies to compensate for different energy calibration. Crosses are data by Hardie *et al.*² Errors are shown where they exceed the size of the symbols. Lines merely connect data points. Scales are linear and have suppressed zeros.

therefore, energy) at which they were scattered. As shown in Ref. 12, such thick-target spectra are easily transformed into differential excitation functions.

The construction of a thick O^{16} target presented some experimental problems. Ice, water, and LiOH targets were used initially, but none was sufficiently uniform or stable under bombardment for the experimental accuracy desired. Finally a high-pressure gas target was built, which in most respects proved satisfactory. The main drawback was that the protons had to pass twice through a relatively thick (0.002-in.) steel window, and straggling and multiple small angle scattering reduced the angular and energy resolution of the thick-target data.¹³ In addition, the background caused by inelastic scattering from the steel window could not easily be corrected for. Typically, the energy resolution obtained for the thick gas target was about 300 keV, and the angular resolution $\Delta\theta = \pm 2^\circ$.

A thick-target survey for elastic excitation functions was made for $13 < E < 18.5$ MeV at the angles $\theta_{lab} = 80, 100, 120, 140, 160^\circ$. This survey revealed a number of very pronounced if broad (≈ 500 keV) fluctuations. Interest in optical-model analysis of $O^{16}(p,p)O^{16}$ scattering and the experimental usefulness of good absolute cross sections prompted us to supplement this initial survey by conventional thin-target cross section measurements, as described in the first paragraph. Thin

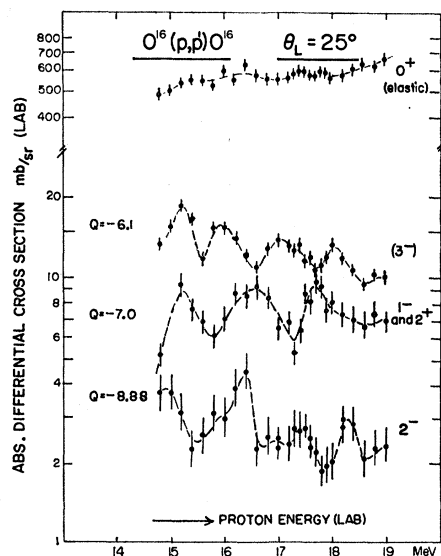


FIG. 5. Elastic and inelastic excitation functions at $\theta_{lab} = 25^\circ$, plotted on log scales. Elastic-scattering cross sections at this angle fluctuate by about 10% while inelastic cross sections fluctuate by nearly a factor of 2. The Q value of the level near 8.9 MeV is taken from the literature [T. Lauritsen and F. Ajzenberg-Selove, *Nuclear Data Sheets—Energy Levels of Light Nuclei—May 1962* (National Academy of Sciences—National Research Council, Washington, D. C., 1962), NRC 61-56], the other values are measured.

¹³ The thick targets were constructed by J. Christensen, who also accumulated the thick-target data for $O^{16}(p,p)O^{16}$.

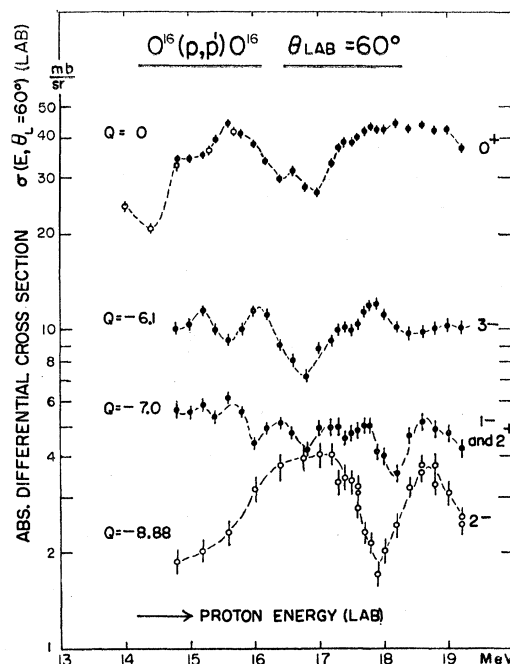


FIG. 6. Elastic and inelastic excitation curves at $\theta_{lab} = 60^\circ$ (near first elastic diffraction minimum). Elastic fluctuations now also reach factor of two.

target measurements provided better angular and energy resolution in addition to absolute values for elastic and inelastic cross sections. Therefore, in the final analysis the thick-target data were not normalized internally as in Ref. 12; rather the absolute cross-section normalization for each thick-target run (covering a range of about 1.5 MeV) was obtained by comparison to our thin-target data for the corresponding interval. All thick-target cross sections so obtained are included in Figs. 3–8. In Table I, thick-target cross sections are given only for energies where no thin-target data were taken.

III. EXPERIMENTAL ERRORS

Energy Resolution and Errors

The cross sections reported in this paper were obtained with various experimental arrangements, and resolution and errors are not quite uniform. The largest energy errors pertain to the thick-target data which are included in Fig. 4, but are not generally tabulated. Typically their energy resolution was about 300 keV while the absolute values of the mean scattering energy were measured with a range-energy device¹⁴ to an accuracy of ± 100 keV.

For thin-target runs the energy resolution was $130 < \Delta E < 180$ keV and mostly a function of the cyclotron performance. The mean bombarding energy was measured with the previously mentioned range-energy

¹⁴ G. Schrank, *Rev. Sci. Instr.* **26**, 677 (1955).

TABLE I. Experimental cross sections for $O^{16}(p,p)O^{16}$ in the laboratory system. Angles in degrees, differential cross sections in mb/sr.

$E_{lab} \backslash \theta_{lab}$	15°	25°	35°	45°	50°	60°	70°	80°	90°	100°	110°	120°	130°	140°	150°	160°
14.8	1460	493	175	39.6	28.7	34.6	46.7	48.1	41.7	37.3	31.2	23.4	17.8	20.3	32.7	50.8
15.0	1400	507	163	38.1		34.9		46.5		30.0		19.5		18.7		47.6
15.2	1513	548	186	37.8	23.0	36.0	51.3	48.3	33.4	22.2	15.8	13.5	14.7	18.7	26.4	36.6
15.4	1540	560	182	37.2		39.7		48.5		19.2		10.3		18.5		31.4
15.6	1493	551	158	28.8		44.9	64.8	58.2	35.9	18.5	10.2	10.7	15.2	19.7	22.8	24.7
15.8	1480	532	163	28.8		42.0		59.0		18.6		6.5		17.8		17.3
16.0	1479	600	166	31.5		38.4	60.8	58.2	40.2	20.0	7.91	4.77	9.00	14.5	17.5	16.8
16.2	1511	558	196	33.7		34.0		53.0		20.2		4.40		13.0		17.4
16.4	1540	634	199	36.7		29.9	46.4	51.0	38.4	21.8	8.74	4.06	5.40	9.11	14.1	17.7
16.6		581	179	42.3		31.7		46.0		19.5		4.35		7.85		16.0
16.8	1490	564	169	40.1		28.0	43.4	43.2	33.3	17.1	6.57	3.03	4.51	7.43	9.89	11.2
17.0	1370	560	184	45.5	25.2	27.2	42.5	40.8	31.6	20.5	10.3	4.42	3.37	5.72	8.61	10.6
17.2	1433	564	200	47.9		33.3		39.5		20.0		6.00		7.20		14.1
17.3	1450	584	190	44.9		37.4	47.2	42.8	31.1	20.2	11.4	6.68	6.27	8.80	13.3	16.6
17.4	1470	602	183	48.5		38.6		42.0		20.5		6.50		8.90		17.6
17.5	1420	600	178	40.2		39.1		45.0		20.0		6.40		9.40		18.0
17.6	1420	582	182	40.8	29.2	40.6	51.7	45.8	30.9	17.1	9.00	5.43	6.59	9.98	14.3	17.1
17.7	1406	578	186	40.2		42.2		46.0		17.2		4.90		8.15		17.5
17.8	1464	599	189	45.2		43.1		42.5		18.0		5.25		7.20		17.6
17.9	1466	598	191	39.3		42.5				19.0		5.05		6.40		17.9
18.0	1440	567	182	39.9	25.6	43.0	53.5	43.4	28.2	16.4	9.24	5.08	3.63	5.83	11.0	17.9
18.2	1424	580	176	36.2		44.8				15.0		5.55		5.55		16.5
18.4	1520	614	184	34.9	25.0	43.2	52.7	44.9	24.0	12.3	7.21	4.80	3.61	4.59	7.79	13.1
18.6	1529	637	186	35.1		43.8										10.8
18.8	1493	631	185	34.0		42.6	51.2	40.3	21.9	9.68	5.29	4.31	3.68	3.60	5.31	8.90
19.0	1530	669	181	35.3		42.8										7.67
19.2	1444			38.1	24.5	37.2	50.8	40.7	23.3	9.16	3.90	3.70	3.59	3.39	3.36	4.78
Relative error	5%	3.5%	5%	7%	10%	3%	3%	3%	2.5%	2.5%	3%	2.5%	2.5%	2.5%	2.5%	2.5%

device to ± 50 keV and regulated to $\pm 0.1\%$. A cross check for the accuracy of the absolute energy determination was made by remeasuring the excitation curve for $O^{16}(p,p)O^{16}$ for $\theta = 160^\circ$ and $16.7 < E < 17.5$

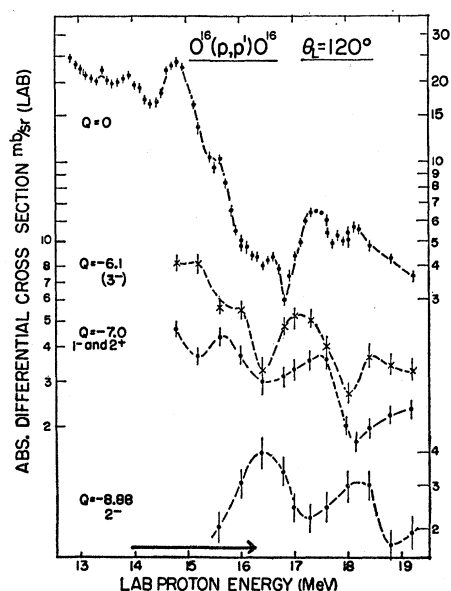


FIG. 7. Elastic and inelastic excitation functions at $\theta_{lab} = 120^\circ$. Recently a similar elastic excitation curve was measured with a smaller beam energy spread (≈ 50 keV) [R. A. Kenefick, W. S. Gray, and J. J. Kraushaar, Bull. Am. Phys. Soc. 9, 68 (1964)].

MeV with a magnetically analyzed beam with a total energy resolution of 60 keV¹⁵ (crosses in Fig. 8). The position of the sharp minimum near 17.0 MeV agrees very well within the quoted errors of the two independent measurements. Cross sections below 15.7 MeV can be compared with data by Kobayashi⁶ (Figs. 3, 4, 8, and 9). The agreement is excellent except for a systematic difference of about 100 keV in the energy scales. This difference is smaller than the sum (125 keV) of the experimental uncertainties reported. It becomes smaller yet if the same range-energy curves are used for the determination of the beam energy. For instance for a range of 385 mg(Al)/cm² more recent curves¹⁶ give an energy $E = 16.00$ MeV while the curves used by Kobayashi¹⁷ yield 15.96 MeV. Our remaining difference in energy scale is about 60 keV, and well within the combined experimental uncertainties. Comparison with another set of published $O^{16}(p,p)O^{16}$ cross sections⁷ with regard to the energy scale is possible but somewhat ambiguous, since the cross sections are given for different back angles. It appears, however, that the energy scale of Ref. 7 differs by about 200 keV from ours and by about 300 keV from Kobayashi's.⁶

¹⁵ The Princeton beam analyzing magnet was recalibrated by R. Pollock to $\Delta E \lesssim \pm 30$ keV. The author is indebted to Ch. Whitten for performing the cross check with the analyzed beam.

¹⁶ Our range energy values for Al were taken from H. Bichsel, Phys. Rev. 112, 1089 (1958); and (private communication 1961).

¹⁷ H. Bichsel, R. F. Mozley, and W. A. Aron, Phys. Rev. 105, 1788 (1957).

Cross-Section Errors

Uncertainties in the differential cross sections are due to counting statistics (<2% for elastic scattering), the need for background (or C¹²) subtraction, counting loss corrections, imperfect reproducibility of energy settings, uncertainties in counter geometry and in charge and angular readings. These errors were estimated and added as random errors, and are given at the bottoms of Tables I-IV. In addition to the errors quoted, we may have unknown systematic errors due to possible faults in target uniformity, charge integration, and zero-angle calibration. The angular calibration error is ±0.2°. Systematic cross-section errors are believed to be smaller than 5% at θ_{lab} = 15° and smaller than 3% for all other angles. For comparison with other work such systematic uncertainties should be added to the explicitly quoted random errors.

In the energy range investigated comparisons with results from Ref. 2 at 13.0 MeV and Refs. 6 and 7 at several other energies can be made and are shown in various figures. Wherever variations of differential cross sections with energy are small we find the expected agreement with all references quoted. In strongly energy-dependent regions, agreement remains good with Refs. 2

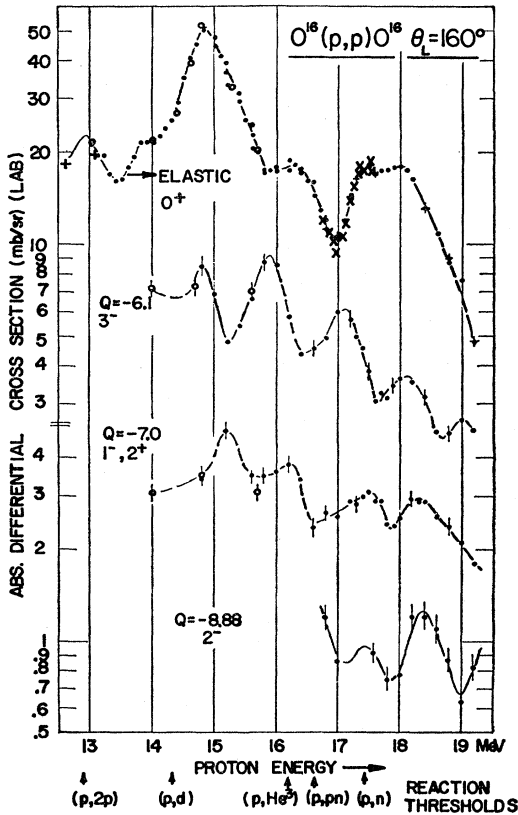


FIG. 8. Elastic and inelastic excitation functions at θ_{lab} = 160° (solid dots). Open circles are values taken from Ref. 6. Crosses are high-resolution data with ΔE < 60 keV (Ref. 15). The threshold energies for various nuclear reactions are shown below the energy scale.

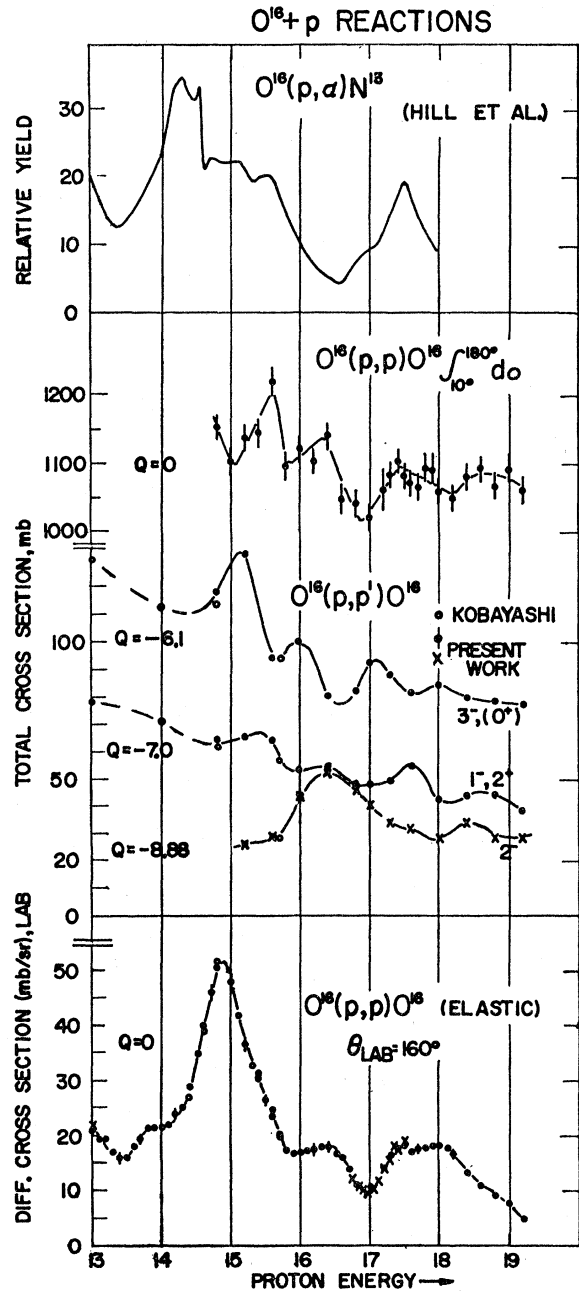


FIG. 9. Comparison of total cross sections for O¹⁶(p,α)N¹⁵ (Ref. 30) with total cross sections for inelastic scattering. Open circles are data by Kobayashi (Ref. 6). Solid dots and crosses refer to present work. Partial cross sections are shown for elastic scattering. Proton energies and excitation energies are in MeV.

and 6. But discrepancies with Ref. 7 of up to 20% appear, which are outside the combined experimental errors and possibly due to a different energy calibration.

IV. DISCUSSION OF ELASTIC-SCATTERING RESULTS

Differential cross sections in the laboratory system for elastic and inelastic scattering are presented in

TABLE II. Experimental cross sections for $O^{16}(p,p')O^{16*}$ (6.1 MeV) in the laboratory system. Differential cross sections in mb/sr, angles in degrees.

$E_{lab} \backslash \theta_{lab}$	15°	25°	35°	45°	50°	60°	70°	80°	90°	100°	110°	120°	130°	140°	150°	160°
14.8		13.6		10.8	10.5	10.2	9.5	8.2	7.9	7.4	8.1	8.3	8.9	8.7	8.7	8.5
15.0		15.8		12.2		10.6										6.9
15.2		19.1		14.1	13.2	11.6	10.8	10.0	9.9	9.6	8.2	8.2	7.2	6.3	5.3	4.8
15.4		17.0		13.1		10.2										5.4
15.6		12.0		11.7	10.1	9.4	7.9	6.0	5.8	5.7	5.6	5.6	5.3	5.5	5.7	6.6
15.8		15.7		13.3		10.1										8.8
16.0		15.7		14.8		11.6	9.6	7.2	5.9	5.0	5.3	5.5	6.0	6.7	7.6	8.6
16.2		14.3		12.3		11.3										5.8
16.4		12.4		10.7		9.0	7.7	6.3	5.2	3.67	3.48	3.28	3.51	3.66	4.06	4.41
16.6		11.2		9.4		8.1										4.57
16.8		13.1	12.0	9.6		7.2	6.0	5.4	4.7	5.0	4.47	4.85	4.69	4.34	4.63	4.90
17.0	13.9	14.0	13.0	12.0	10.8	8.8	6.9	5.4	5.1	5.1	5.9	5.2	5.3	5.2	5.6	6.0
17.2		13.4		12.9		9.3										5.7
17.3		12.8		12.0		10.0	7.3	5.3	4.80	4.87	4.62	5.0	4.86	4.79	4.55	5.0
17.4		13.5		12.7		10.2										4.58
17.5		11.6		11.8		10.0										3.85
17.6		11.9		11.5	11.5	10.5	8.8	6.5	3.93	2.96	3.34	3.97	4.49	4.19	3.91	3.06
17.7		10.8		12.3		11.5										3.29
17.8		11.3		13.2		12.1										3.13
17.9		12.1		13.1		12.2										3.46
18.0		13.4		11.9	11.0	11.2	9.1	7.2	4.89	3.08	2.01	2.69	3.24	3.77	4.14	3.63
18.2		12.0		11.6		10.3										3.56
18.4		10.7		10.9	10.2	9.8	8.2	7.0	5.2	4.11	3.79	3.64	3.37	3.46	3.43	3.18
18.6		9.6		10.2		9.8										2.42
18.8		10.4		11.9	11.5	10.1	7.8	6.5	4.62	3.52	3.46	3.40	3.53	3.43	2.80	2.40
19.0		10.1		12.3		10.4										2.69
19.2	9.7				10.9	10.3	8.4	6.2	4.58	3.34	3.27	3.27	3.30	3.30	3.04	2.47
Relative error	10%	5%	10%	6%	5%	4%	5%	5%	4%	5%	5%	5%	5%	5%	5%	5%

TABLE III. Experimental cross sections for $O^{16}(p,p')O^{16*}$ (7.0 MeV) in the laboratory system. Differential cross sections in mb/sr, angles in degrees.

$E_{lab} \backslash \theta_{lab}$	15°	25°	35°	45°	50°	60°	70°	80°	90°	100°	110°	120°	130°	140°	150°	160°
14.8		5.17			5.5	5.7	6.4	5.5	5.6	5.2	5.2	4.7	4.0	3.9	3.7	3.4
15.0		7.4				5.6										
15.2		9.6			7.0	6.0	5.4	5.0	5.0	4.8	4.2	3.7	3.2	3.2	3.8	4.9
15.4		7.8				5.4										
15.6		7.0	8.0		6.4	6.2	5.4	4.7	4.8	4.6	4.1	4.4	4.3	4.2	3.8	3.5
15.8		6.2				5.7										3.5
16.0		7.1				4.5	4.3	3.4	3.2	2.89	3.1	3.7	4.1	4.5	4.2	3.6
16.2		8.9		8.3		5.0										3.8
16.4		8.7		8.3		5.2	3.8	2.71	2.83	2.60	2.62	3.0	3.42	3.5	3.6	3.4
16.6		9.5		8.6		4.8										2.37
16.8	5.5	8.5	9.0	7.9		4.2	2.74	2.15	2.40	2.40	2.78	3.1	3.1	2.90	2.77	2.67
17.0	4.5	6.6	7.7	7.0	5.8	5.0	3.8	2.46	2.21	2.26	3.1	3.3	3.4	3.4	3.0	2.57
17.2		6.9		6.2		5.0										2.88
17.3		5.3		6.5		5.0	3.6	3.2	2.68	2.81	3.7	3.6	3.8	3.5	3.3	2.81
17.4		6.4		6.8		4.6										2.95
17.5		8.7		6.6		4.8										3.07
17.6		8.2	7.9	7.3	7.2	4.9	3.7	2.79	3.0	3.3	3.6	3.6	3.1	2.91	2.83	2.89
17.7		9.9		8.3		5.1										2.89
17.8		9.4		7.9		5.2										2.42
17.9		7.6		6.8		4.2										2.39
18.0		8.2		6.1	5.7	4.1	2.57	2.18	2.35	2.34	2.12	1.78	1.50	1.45	1.95	2.53
18.2		7.3		6.7		3.6										
18.4		7.0		7.3	7.0	4.7	3.0	2.09	1.93	2.14	2.07	1.96	1.88	1.93	2.39	2.88
18.6		6.6		8.2		5.2										2.54
18.8		7.4	8.8	7.0	6.8	4.9	3.2	2.14	1.95	2.04	2.36	2.21	2.08	1.97	2.09	2.39
19.0		7.0		6.9		4.8										2.10
19.2	3.9				5.6	4.3	2.73	1.80	1.96	2.07	2.77	2.33	2.06	1.91	1.88	1.78
Relative error	20%	10%	15%	8%	6%	5%	6%	6%	5%	6%	6%	5%	6%	6%	6%	5%

TABLE IV. Experimental cross sections for O¹⁶(*p, p'*)O^{16*} (8.88 MeV) in the laboratory system. Angles in degrees, differential cross sections in mb/sr.

$E_{\text{lab}} \backslash \theta_{\text{lab}}$	15°	25°	35°	45°	50°	60°	70°	80°	90°	100°	110°	120°	130°	140°	150°	160°
15.0		3.6														
15.2		3.2				2.0	2.6	2.4	2.9	2.3						
15.4		2.3														
15.6		2.6				2.4	2.5	3.2	2.9	2.9	2.3	2.1				
15.8		3.1														
16.0		3.0				3.3	3.8	4.1	4.6	4.1	4.0	3.1	2.8	2.7	1.8	
16.2		3.9		3.0												
16.4		4.5		3.0		3.9	4.7	5.8	5.7	6.0	4.8	4.0	3.0	2.4	2.1	
16.6		2.3		2.6												
16.8	2.7	2.5	2.8	3.2		4.1	4.7	4.9	5.7	5.2	4.7	3.4	2.2	1.8	1.4	1.2
17.0	1.7	2.6	3.2	3.8	3.7	4.0	4.7	4.6	4.3	3.7	3.4	2.5	1.9	1.4	1.0	0.86
17.2		2.4		3.2		4.1										
17.3		2.7				3.3	3.6	3.9	3.6	3.3	2.6	2.3	1.9	1.5	1.1	
17.4		2.7				3.5										
17.5		2.8				3.4										
17.6		2.4	2.7		3.1	3.0	2.7	3.1	3.0	3.1	2.6	2.5	2.0	1.7	1.3	0.92
17.7		2.3				2.4										
17.8		1.9	2.6			2.2										0.75
17.9		2.0				1.7										
18.0		2.0	2.5		1.9	2.0	2.1	2.1	2.4	2.8	2.9	3.0	2.6	2.1	1.5	0.77
18.2		2.9	3.2			2.5										1.2
18.4		2.9	3.3		3.5	3.1	2.9	2.5	2.3	2.7	2.7	3.0	2.9	2.3	1.5	1.2
18.6		2.1	2.9			3.7										1.1
18.8		2.3	3.0		3.0	3.5	2.8	2.9	2.4	2.5	2.0	1.7	1.7	1.5	0.85	0.87
19.0		2.4	3.0			3.0										0.63
19.2	2.9				2.5	2.6	2.9	2.7	2.8	2.7	2.1	2.0	1.7	1.3	1.0	0.82
Relative error	20%	15%	20%	10%	10%	10%	10%	10%	10%	10%	10%	10%	10%	15%	15%	10%

Tables I–IV. The numerical values given were usually taken from the thin-target runs and often represent weighted averages of more than one measurement. The tabulated differential cross sections can be viewed either as closely spaced angular distributions or as excitation functions, with the same relative (random) errors in either view. A comparison of our data with that of several other experiments is given in Fig. 3. Graphical presentations of most of the present data are given in Figs. 3–8.

A study of our experimental cross sections (Fig. 4) reveals fluctuations that are both much narrower and more pronounced than those expected from optical-model resonances in this energy region (compare with Ref. 12). On the other hand, we no longer have isolated compound nucleus resonances, but strongly interfering ones. This makes a quantitative analysis of the experiment very difficult. If the level density in the compound nucleus F¹⁷ were high enough, a statistical interpretation of the cross-section fluctuations¹⁸ might be attempted. Two facts speak against using this interesting approach for this experiment: (a) For many of the fluctuations reported here, the experimental energy resolution is comparable to the width rather than much narrower, and existing theoretical formulas would have to be modified accordingly. (b) The theoretical assumption of very high level density for levels of the same spin and parity

is probably not justified in F¹⁷ for $-13 > Q > -19$ MeV. Well-isolated narrow (< 5 keV) levels in F¹⁷ have been observed as high as $Q = -13.034$ MeV.²

In view of the continued success of the optical-model approach for heavier nuclei, it seemed necessary to investigate to which extent conventional optical-model analysis of O¹⁶(*p, p'*)O¹⁶ could explain the dominant features of the elastic scattering in this energy region. Duke⁹ made a very complete O¹⁶(*p, p'*)O¹⁶ analysis, which included data obtained by Kobayashi⁶ (for $8.66 < E_p < 15.6$ MeV), and by this author ($15.2 < E < 19.2$ MeV) as well as polarization results available for a lower energy (10 MeV).¹⁹ It was found that without changes in the optical-model parameters from energy to energy only extremely rough fits to the data could be obtained. Similarly fits with only two energy-dependent parameters (*V, W*) remained unsatisfactory for O¹⁶. In order to reproduce all experimental data to within at least a few standard deviations, five or more parameters had to be varied. Duke's analysis showed that the variation of six optical-model parameters within physically reasonable limits permits us to fit all experimental angular distributions to within about 10% or better.⁹ The actual range of the parameters was $0.3 < a < 0.6F$, $0.2 < b < 1.4F$, $43 < V < 53$ MeV, $0 \leq W \leq 4$ MeV, $1 < W_1 < 28$ MeV, and $2.3 < V_s < 12.3$ MeV. We would draw these conclusions from Duke's work: It is possible to obtain fairly good

¹⁸ T. Ericson, Phys. Letters 4, 258 (1963), and P. A. Moldauer, *ibid.* 8, 70 (1964), and references therein.

¹⁹ L. Rosen, J. E. Brolley, Jr., and L. Stewart, Phys. Rev. 121, 1423 (1961).

fits at any one particular energy with physically "reasonable" parameters. But the need for rapid parameter variation with energy shows that the conventional optical-model picture for scattering of protons by O^{16} (and also¹¹ by C^{12}) is a considerable oversimplification. For O^{16} it is not safe to assume that fitting parameters obtained at one particular energy will be similarly useful at nearby energies, or that one good optical-model fit is sufficient proof for the 'direct' nature of the interaction. From the practical point of view Duke's paper has left us with a very useful parameterization of a large amount of experimental data. Since his fits to the data are so close, his published parameters permit the convenient derivation of good scattering phase shifts and wave functions for DWBA calculations in the region $8.7 < E_p < 19.2$ MeV.

It is clear from the early work of Feshbach, Porter, and Weisskopf²⁰ that the optical model cannot account for compound-nucleus contributions to elastic scattering. The very limited success of the straightforward optical-model analysis of $O^{16}(p,p)O^{16}$ emphasizes the fact that we cannot ignore compound effects. Thus, some criticism²¹ of Duke's approach has had the implication that the compound-nucleus contributions to the scattering cross section should be and could be eliminated before an optical-model analysis is made. There is no doubt that it is desirable to eliminate or avoid compound-nucleus effects. We feel, however, that for light nuclei in the energy region under discussion, at present there is no easy way to do so, and we shall try to show why. Some experimenters hope to avoid the problem by analyzing data only for angular or energy regions which do not exhibit strong compound-nucleus contributions. Others calculate compound cross sections (by Hauser-Feshbach theory²²) and subtract them from the observed cross sections. There are indeed special situations where one or the other method is successful. For instance, if in the compound nucleus all levels, which can be excited, have widths Γ much smaller than their spacing D , $\Gamma \ll D$, there will be energy regions, between resonances, where scattering is pure potential scattering. This often happens in light nuclei for very low bombarding energies. The other extreme of very high level density in the compound nucleus where $D \ll \Delta E$ (ΔE = spread in bombarding energy) can be attacked, by subtracting the predicted compound-nucleus contribution. Cranberg²³ have obtained beautiful optical-model fits to low-energy (≈ 4 MeV) neutron scattering in the lead region, in this fashion.

In the case of light nuclei with $10 < E_p < 20$ MeV the experimental situation does not fulfill the conditions for either of the above methods. The level widths are of

the same order of magnitude as the level spacing, or broader, and there are no regions of pure potential scattering. On the other hand, our ΔE covers only a relatively small number of levels, and so simple subtraction of a compound-nucleus cross section is not possible. In the paper by Hardie *et al.*² optical-model fits (V , W variable) for $O^{16}(p,p)O^{16}$ are shown for proton energies from 8.5 to 13 MeV. Most fits were calculated for energies as far as possible removed from pronounced resonances ($E_p = 13.048, 11.897, 11.297, 10.196, \text{ and } 9.495$ MeV). Some are for energies close to (within Γ) noticeable fluctuations ($E_p = 12.597, 10.744, 8.993, 8.495$ MeV). Neglecting the fit at $E_p = 8.993$ MeV, which is particularly poor, one would be justified in saying that the quality of the fits decreases with decreasing energy, and does not depend on the closeness of a resonance. A disagreement of many standard deviations between data and fits generally appears at angles as low as 60° . This supports our contention that for O^{16} fluctuations due to compound-nucleus effects cannot be avoided by restricting the analysis to forward angles and/or "quiet" energy regions. A look at our data in the 13–19-MeV region (Figs. 4–9) reveals no energy region free of significant fluctuations. Neither do we see a smooth variation of cross section with energy at forward angles. In fact it is easy to show that averaging over 200 keV hardly suppresses any structure that one might expect from the interference of direct and compound scattering terms:

We may write the elastic-scattering amplitude as $T = T_D + T_C$, where T_D stands for the part of T that varies very slowly with energy, and T_C for the strongly energy-dependent part. We can think of T_D as similar to the constant-parameter optical-model prediction. (See, for instance, Ref. 12, Fig. 9.) We then can write for the differential scattering cross section

$$\sigma(\theta) = |T|^2 = |T_D|^2 + \text{Re}(T_D^* T_C + T_C^* T_D) + |T_C|^2. \quad (1)$$

Our 200-keV spread in the beam energy allows the excitation of various levels (presumably 10–100) in the compound nucleus F^{17} . If the number of contributing levels is large enough to satisfy the statistical assumptions for calculations of the Hauser-Feshbach²² type, the interference term should average to zero. Hence $\sigma = \sigma_D + \sigma_C$. Consequently the fluctuations, defined as $\Delta\sigma = \sigma - \sigma_D$, would be subject to the inequality

$$0 \lesssim \Delta\sigma \lesssim \sigma_C, \quad (2)$$

because $\sigma_C = |T_C|^2$ is always positive. Since Hauser-Feshbach cross sections have angular symmetry about $\theta_{\text{c.m.}} = 90^\circ$ we can find an upper limit for σ_C by assuming $\sigma_C(\theta) \leq \sigma(180 - \theta)$ for small values of θ , where we take σ and θ in the c.m. system. Let us, as a test, compare $\Delta\sigma(\theta_{\text{c.m.}} = 26.4^\circ)$ and $\sigma(\theta = 153.6^\circ)$. If a statistical approach is valid, we should find for the amplitude of

²⁰ H. Feshbach, C. E. Porter, and V. F. Weisskopf, Phys. Rev. **96**, 448 (1954).

²¹ Discussions at Gatlinburg, Conference on Compound Nuclear States, 1963 (unpublished).

²² W. Hauser and H. Feshbach, Phys. Rev. **87**, 366 (1952) and L. Wolfenstein, *ibid.* **82**, 690 (1951).

²³ L. Cranberg (to be published).

fluctuations at $\theta = 26.4^\circ$, for instance, that

$$\Delta\sigma(26.4^\circ) \leq \sigma(153.6^\circ). \quad (3)$$

From Table I or Fig. 4 we find near 16.4 MeV $\Delta\sigma(26.4^\circ) \approx 70$ mb/sr and $\sigma(153.6^\circ) \approx 16.3$ mb/sr. Near 19 MeV we find $\Delta\sigma(26.4^\circ) \approx 45$ mb/sr and $\sigma(153.6^\circ) \approx 5.6$ mb/sr. These examples severely violate inequality (3). It is easy to find many other such violations at other energies and angles, and also for C¹²(p, p)C¹² (Ref. 12). This indicates both that the prerequisites for a Hauser-Feshbach calculation are not present for O¹⁶, and that less sophisticated methods for the subtraction of compound nucleus effects are certainly doomed to failure.

We can easily discuss the general case where the interference term contributes to the fluctuations.

Here

$$\Delta\sigma = |T|^2 - |T_D|^2 = \sigma_C + 2\text{Re}(T_D T_C^*) \quad (4a)$$

or

$$(\Delta\sigma - \sigma_C)^2 = 4\{\text{Re}(T_D T_C^*)\}^2. \quad (4b)$$

In order to find an upper limit for the magnitude of the interference term, we recall that for any complex number A , $AA^* = (\text{Re}A)^2 + (\text{Im}A)^2$. Therefore,

$$\{\text{Re}(T_D T_C^*)\}^2 = (|T_D|^2 |T_C|^2 - [\text{Im}(T_D T_C^*)]^2)$$

or

$$\{\text{Re}(T_D T_C^*)\}^2 \leq \sigma_D \sigma_C$$

and hence

$$(\Delta\sigma - \sigma_C)^2 \leq 4\sigma_D \sigma_C$$

or

$$|\Delta\sigma - \sigma_C| \leq +2(\sigma_D \sigma_C)^{1/2}, \quad (5)$$

where σ_D and σ_C are always real and positive, while $\Delta\sigma$ now may have either sign. This relation is quite general, because it is only based on quantum mechanics and not on any particular reaction model. The inequality can be compared with experiment if we can estimate σ_C . Outside the statistical approach we cannot, in general, expect symmetry with respect to 90° for compound-nucleus contributions. But we may assume that in a large energy interval, for instance from 16 to 19 MeV, compound-nucleus contributions will be about equally as often backward peaked as forward peaked. We may then predict for instance, that for $\theta_{e.m.} = 26.4^\circ$ the largest compound-nuclear cross section is limited by the relation $\sigma_{C_{\max}}(26.4^\circ) \approx \sigma_{C_{\max}}(153.6^\circ) < \sigma_{\max}(153.6^\circ) \approx 20$ mb/sr, and may compare this number according to Eq. (5) with the largest fluctuations at $\theta_{e.m.} = 26.4^\circ$, which are about ± 40 mb/sr. Inserting,

$$|\Delta\sigma - \sigma_C| = |\pm 40 - 20| \lesssim 2(540 \times 20)^{1/2} = 208 \text{ mb/sr}.$$

Now inequality (5) is well obeyed as it must be. We can make a similar comparison for the high-resolution data of Ref. 2, for instance, for $9.5 < E_p < 13$ MeV. There $\Delta\sigma_{\max}(28^\circ) = \pm 60$ mb/sr, and $\sigma_{\max}(152^\circ) \approx 40$ mb/sr. Hence

$$|\Delta\sigma - \sigma_C| \approx |\pm 60 - 40| \lesssim 2(375 \times 40)^{1/2} = 245 \text{ mb/sr}.$$

TABLE V. Locations and widths of fluctuations.

E_p (lab) (MeV) ± 0.1	Approximate width (keV)	Resonating group $-Q$ (MeV)
13.35	400-500	0
13.9	200-500	0
14.85	600-800	0, 6.1
15.1	500-700	6.1
15.5	400-700	0, 6.1, 7.0, 8.88
15.9	400-700	0, 6.1
16.4	300-500	0, 6.1, 7.0, 8.88
16.9	500-600	0
17.1	300-600	6.1
17.45	300-600	0 7.0
17.6	400-600	7.0
17.9	300-600	0, 7.0, 8.88
18.15	300-600	0, 6.1
18.4	300-700	7.0, 8.88
19.0	300-500	0, 6.1, 8.88

Another comparison is possible for C¹²(p, p)C¹² data between 14 and 19 MeV (Ref. 12). Since accurate data are given for $\theta_{e.m.} = 16^\circ$, we shall make our analysis for 16 and 164° . $\Delta\sigma(16^\circ) = \pm 90$ mb/sr, and $\sigma_{\max}(160^\circ) = 19$ mb/sr. Therefore

$$|\Delta\sigma - \sigma_C| \approx |\pm 90 - 19| \lesssim 2(780 \times 19)^{1/2} = 244 \text{ mb/sr}.$$

In our examples the high-resolution data ($\Delta E < 5$ keV) for O¹⁶ as well as the 200-keV resolution data for C¹² and O¹⁶ have fluctuations that reach about 30-45% of the predicted maximum values, for the energy regions considered. If we recall that we overestimated both σ_C and the real part of the interference term, we may conclude that the interference term contributes almost in maximum strength, and is hardly reduced by the 200-keV energy averaging.

As in the case of C¹² the phase shifts for O¹⁶(p, p)O¹⁶ scattering ($13 < E_p < 19$ MeV) indicate interfering rather than isolated resonances.²⁴ The strongest resonances in the elastic channel are seen near $E_p = 13.35, 14.85,$ and 16.9 MeV. Generally, only locations and approximate widths of large fluctuations can be pointed out (Table V). There is a more sophisticated approach for the treatment of elastic scattering from light nuclei which involves the inclusion of one²⁵ or more²⁶ resonant terms in the scattering amplitude in addition to the optical-model term. Easlea²⁵ succeeded in improving fits at and near the 10.5-MeV O¹⁶(p, p)O¹⁶ resonance, but could not fully eliminate the energy dependence of the optical-model parameters. Since later optical-model work⁹ indicates no particular fitting trouble near 10.5 MeV, Easlea's success permits no definite conclusions. Tamura²⁶ has used 3 resonant terms to fit 4 excitation functions ($\theta_L = 43^\circ, 56.5^\circ, 132^\circ, 142^\circ$) for C¹²(p, p)C¹², for proton energies of $20 < E_p < 30$ MeV. After thus introducing 12 new parameters, he was able to predict

²⁴ C. B. Duke (private communication).

²⁵ B. Easlea, University of London, Ph.D. thesis, 1961 (unpublished).

²⁶ T. Tamura and T. Terasawa (to be published).

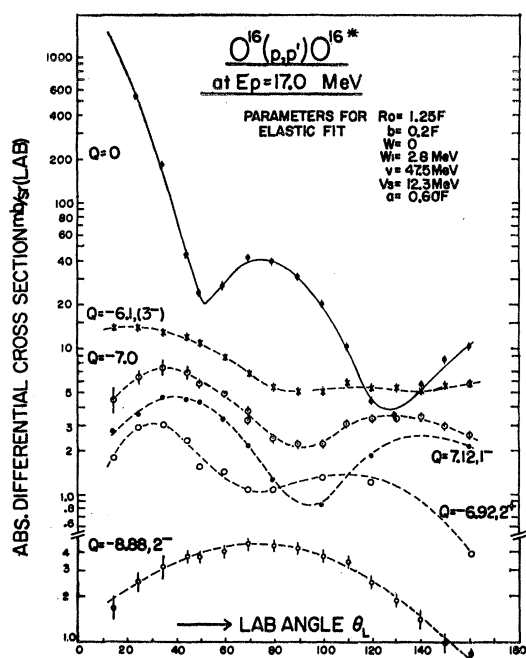


FIG. 10. Angular distributions for elastic and inelastic scattering of 17-MeV protons. Points with error marks are taken from Tables I-IV. The curves labeled $Q = -7.12, 1^-$ and $Q = -6.92, 2^+$ are obtained by graphical analysis of the partially resolved $Q = -7.0$ -MeV doublet (see Fig. 2). These curves have systematic errors, which are hard to assess, but certainly larger than the random errors shown for the sum curve, $Q = -7.0$ MeV. Dashed curves are drawn to connect data points. The solid line is an optical-model fit to the elastic data (Ref. 9).

correctly the general trend of the angular distributions for $20 < E_p < 30$ with constant optical-model parameters. His method has not yet been applied to energies below 20 MeV or to O^{16} .

The most satisfying quantitative theoretical approach to scattering from some light nuclei might possibly be found in recent work by Feshbach²⁷ and Lemmer.²⁸ These authors extend the conventional one-body-in-a-central-potential approach for scattering to include two-particle or three-particle interactions and thus take explicit account of some easily formed compound states. Calculations have been published²⁸ for $N^{15}(p,p)N^{15}$ excitation functions that show qualitative similarity with our $O^{16}(p,p)O^{16}$ data. Lemmer's approach in this calculation was to represent the N^{15} nucleus by a hole state in a central potential (in analogy to shell-model work) and to consider in addition to potential scattering the interaction between this hole and the incident particle. The work can and possibly will be extended to $O^{16}(p,p)O^{16}$,²⁸ although it will be more complicated than for $N^{15} + p$. For $O^{16} + p$ one assumes that the bombarding particle can create a hole in the closed O^{16} shell by lifting

one nucleon to the empty $d_{5/2}$ shell. The intermediate ("doorway") state can then be represented as a two-particle, one-hole state. Such doorway states are expected to have widths of several hundred keV in the energy region of interest. They may decay into the entrance channel (elastic scattering) or other channels (inelastic processes) thus giving rise to semisharp fluctuations in the elastic as well as inelastic cross sections. The existence of such structure, intermediate between single particle resonances and narrow resonances due to complicated, long-lived compound states has been discussed for some time. In particular, sharp and semisharp states at high energies are expected from the cluster model of nuclei.²⁹ For unbound cluster states Phillips and Tombrello predicted the occurrence of one or more scattering resonances near each free two-cluster parent,²⁹ e.g., for our experiment near the $(p,2p)$, (p,d) , (p,He^3) , (p,pn) , and (p,n) thresholds. We certainly see an abundance of resonances near and above these thresholds (see Figs. 4 to 9). It should be very interesting to further examine the nature of these intermediate states as soon as quantitative theoretical predictions become available.

V. INELASTIC SCATTERING

For experimental reasons (decreasing cross sections, increasing background) data on inelastic scattering are neither as accurate nor as plentiful as those for elastic scattering. But a few comparisons with previous work^{4,6} can be made. As indicated in Fig. 3 agreement with the present work is generally good. Hence, it is quite certain that inelastic scattering from O^{16} also shows strong energy dependence (Figs. 5-9), even for the total cross sections (Fig. 9), and for bombarding energies as high as 19 MeV. Particularly strong resonances are seen for the $2^-, Q = -8.88$ -MeV state near 16.4 and 18.4 MeV. For the $Q = -6.1$ -MeV group, which is mostly due to the 3^- state at 6.13 MeV, the strongest fluctuations are near 15.1, 15.9, and 17.1 MeV. Various other discernable fluctuations seen mostly for the differential cross section are also listed in Table V. These fluctuations are not isolated and it is difficult to ascertain the corresponding resonance energies and widths. Hence, the energies given in Table V merely serve to identify the larger fluctuations and their apparent widths after correction for the finite spread in bombarding energy.

In Fig. 9, we compare our proton scattering data with the $O^{16}(p,\alpha)N^{13}$ data reported by Hill *et al.*³⁰ It appears that the very strong fluctuations in the (p,α) and (p,p') reactions do not occur at the same energies. However, some weaker (p,α) fluctuations seem to have counterparts in the (p,p') scattering cross sections. For instance the fluctuations at 13.35 and 16.95 MeV in

²⁷ H. Feshbach, Gatlinburg Conference on Compound Nuclear States, A2, 1963 (unpublished).

²⁸ R. H. Lemmer and C. M. Shakin, Gatlinburg Conference on Compound Nuclear States, A3, 1963 (unpublished), and R. H. Lemmer (private communication).

²⁹ J. A. Wheeler, Phys. Rev. **52**, 1107 (1937). K. Wildermuth and T. Kananopolous, Nucl. Phys. **7**, 150 (1958). G. C. Phillips and T. A. Tombrello, Nucl. Phys. **19**, 555 (1960).

³⁰ H. A. Hill, E. L. Haase, and D. B. Knudsen, Phys. Rev. **123**, 1301 (1961).

elastic scattering and those at 15.5 and 17.45 MeV for scattering to the $(1^-, 2^+)$ doublet near $Q = -7.0$ MeV might be correlated to the $O^{16}(p, \alpha)N^{13}$ cross sections. In the energy region $13 < E < 20$ MeV we have reaction thresholds for (p, d) , (p, He^3) , (p, pn) , and (p, n) at energies shown in Figs. 4 and 8. Again we see no unambiguous correlations with the scattering data; however, Duke⁹ found that his optical-model parameters shifted markedly near the (p, d) and (p, n) thresholds. Angular distributions for elastic and inelastic proton scattering from O^{16} always resemble those shown in Fig. 10. We see forward peaking and asymmetry with respect to $\theta = 90^\circ$ at all energies. Hence direct interactions are most likely the main reaction mechanism, and DWBA calculations for inelastic scattering might be attempted. However, in view of the energy dependence of the cross sections, it is not expected that good detailed agreement with the experimental cross sections will be found. It is interesting to observe (Fig. 10) that scattering from the 4th excited state ($1^-, Q = -7.12$) is about 1.7 times as strong as that to the 3rd excited state ($2^+, Q = -6.92$). Therefore, the angular distributions of the 7.0-MeV proton group roughly resemble the scattering from the 1^- state. Again as for elastic scattering a more satisfying theoretical treatment albeit beyond the scope of this paper might be found in the approach by Feshbach and Lemmer^{27, 28}: by allowing the 2-particle 1-hole "doorway states" to decay to excited states of O^{16} .

VI. SUMMARY

Elastic and inelastic scattering of 14.8–19.2-MeV protons by O^{16} is characterized by strong energy dependence. Differential cross sections frequently change by a factor of 2 or more within 200–500 keV, even at forward angles and for elastic scattering. Table V lists some of the major fluctuations, which are often seen in more than one reaction channel. Angular distributions change less drastically with energy than the excitation functions and generally have shapes similar to the ones predicted by direct interaction models. Good fits to the elastic-scattering cross sections could be obtained by the use of an optical-model search code. However, in view of the nonuniform variation of the optical-model pa-

rameters needed to obtain these fits a more fundamental approach to proton scattering from light nuclei such as O^{16} and C^{12} is desirable. It is felt that calculations like Lemmer's²⁸ for $N^{15}(p, p)N^{15}$ hold some promise for explaining energy dependence as well as angular distributions for proton scattering in this energy region. DWBA calculations for inelastic scattering have not yet been attempted, mainly because of the difficulties mentioned for the optical-model parameters. There are indications^{5, 31} that even at much higher energies (30 MeV) scattering from nuclei like C^{12} and O^{16} is not well described by a one-step direct interaction and that similar effects may be seen in nuclei as heavy as Mg^{24} . Interference of the direct and compound-nucleus scattering amplitudes is very noticeable for $O^{16}(p, p)O^{16}$ below 20 MeV. It was shown in the discussion that our beam spread of 200 keV produced little averaging out of the interference term. This would imply that the density of levels in F^{17} is still quite small for $-13 \geq Q \geq -19$ MeV, or that only special groups of states are easily excited and dominate compound nuclear scattering.

Apart from questions of theoretical interest the data reported for $O^{16}(p, p)O^{16}$ may have some practical uses, such as the generation of wave functions for protons scattered from O^{16} for stripping and polarization calculations, or the experimental use of the measured $O^{16}(p, p)O^{16}$ cross sections, for the determination of absolute cross sections for proton-induced reactions with elements that can be most conveniently obtained in oxide form.

ACKNOWLEDGMENTS

The author wishes to thank J. Cristenson for the construction of the thick gas target and help with data taking and analysis. D. Fong, Ch. Glasshauser, and J. Crawley helped with the processing of the data at various stages of the work. The author wishes to acknowledge helpful discussions with Professor N. Austern, Professor R. Drisko, and Professor R. Lemmer, and to thank Professor R. Sherr for the suggestion of and continued interest in this experiment.

³¹ J. K. Dickens, D. A. Haner, and C. N. Waddell, *Phys. Rev.* **132**, 2159 (1963).